SPE-191433-18IHFT-MS

Acid Fracturing Productivity Model for Naturally Fractured Carbonate Reservoirs

Assiya Ugursal, Mateus Palharini Schwalbert, Ding Zhu, and Alfred Daniel Hill, Texas A&M University

This paper was prepared for presentation at the SPE International Hydraulic Fracturing Technology Conference and Exhibition held in Muscat, Oman, 16 - 18 October 2018.

Abstract

In naturally fractured carbonates, the efficiency of acid fracturing stimulation can be hindered due to the decreased effective length and conductivity of created fractures, and acid loss into natural fractures is one of the main reasons for the reduced efficiency. At the same time, acid that leaks into natural fractures creates additional conductivity that may enhance production from the stimulated well. A model was developed to predict the acid fracturing performance in naturally fractured carbonate reservoir by taking into account the etching of both hydraulically induced and naturally occurring fractures to estimate fracture conductivity and well productivity.

The model uses a domain that contains a well and a rectangular reservoir. The well is intersected by a bi-wing vertical hydraulic fracture which is intersected by transverse natural fractures. The model simulates acid injection into the fracture system, acid-rock reaction, and width increase for both hydraulic and natural fractures. At the end of the acid injection, the conductivity of the fracture system is estimated, and the well stimulation efficiency is evaluated by calculating productivity increase and skin factor. This is done by simulating the production flow into the hydraulic and natural fractures using a coupled reservoir model without the need of an external reservoir simulator. In contrast to previously published acid fracturing models which calculate leakoff using the Carter's model, in this study, we developed a model that calculates the leakoff during acid injection by simulating the flow through porous media using a reservoir model, which includes both hydraulic and natural fractures.

In contrast to the Carter's leakoff model which assumes that fractures are spaced far enough so that no interaction among the fractures occurs, the new approach allows the natural fractures to interact with each other as acid leaks off and pressure changes in the reservoir surrounding the fractures. The new approach does not impose limitations on fracture spacing, and leakoff rate of individual natural fractures is a function of fracture spacing and location. The other feature of the new model is that the leakoff flow rate does not necessarily decrease with time, unlike what Carter's leakoff model predicts. It was observed that leakoff rate from natural fractures may increase initially as the natural fractures are stimulated. The effects of natural fracture geometry and spacing, reservoir permeability, and treatment conditions on acid leakoff, fracture conductivity and well productivity are analyzed. The role of natural fractures on stimulation efficiency is evaluated by comparing the results with the cases where no natural fractures are present in the reservoir.

The model enables a better prediction of acid fracturing performance in naturally fractured carbonate reservoirs, and also simulates more realistic leakoff behavior compared to the conventional leakoff model, which improves the accuracy of the results.

Introduction

A well productivity depends on various parameters, including the formation permeability in the near-wellbore area and in the surrounding reservoir. When the original reservoir permeability is low, a fracturing stimulation is often necessary to maintain efficient production. In carbonate reservoirs, acid fracturing is a feasible option. The objective of acid fracturing treatments is to create long conductive pathways (fractures) to enhance fluid flow from the reservoir into the wellbore. The flowing ability of the fracture created during acid fracturing process is defined by fracture conductivity, which is a product of fracture permeability and fracture width.

In naturally fractured carbonate reservoirs, the physical characteristics of individual natural fractures define the fluid flow properties of the fracture network. The fractures can be either favorable or unfavorable for fluid flow in a reservoir and can affect stimulation efficiency and well productivity in either positive or negative way. The main parameters that determine the fluid flow properties of natural fractures are fracture width, fracture spacing, and interconnectivity of the fractures inside the network. Overall, the permeability of a fracture network increases with increasing fracture width and decreasing fracture spacing.

During the acid fracturing stimulation treatment in a naturally fractured carbonate reservoir, acid injection into formation at a high rate and pressure will induce fractures (main fractures) and will open existing natural fractures. Hydraulically induced fractures are referred to as hydraulic fractures throughout this paper. When the formation contains a large amount of natural fractures, acid fracturing treatments are challenged by an increased acid loss from the hydraulic fracture into the intersecting natural fractures. This can limit the hydraulic fracture growth and reduce the effective fracture length. Also, increased leakoff reduces the amount of acid inside the hydraulic fracture, resulting in a lower conductivity of the hydraulic fracture. Meanwhile, the acid that leaks into the natural fractures reacts with the natural fracture walls, increasing the natural fracture width and generating additional conductivity. There are multiple publications on improving the acid fracturing efficiency in naturally fractured reservoirs, and many of which focus on using viscoelastic acid systems with diverters to reduce the acid loss from the main fractures by bridging the natural fractures (Rahim et al. 2017; Williams et al. 2016; McCartney et al. 2017). However, the effect of leakoff on natural fracture conductivity and efficiency of acid fracturing treatment is not fully understood.

In order to improve the prediction of acid fracturing performance in naturally fractured carbonate reservoirs, a model is required that accounts for conductivity generation in both in hydraulically induced and natural fractures, and estimates post-stimulation productivity based on the overall conductivity of the fracture system. Existing acid fracturing models (Settari et al. 2001; Romero et al. 2001, Mou et al. 2010, Oeth et al. 2014) estimate fracture conductivity by assuming acid flow and reaction in the hydraulic fractures only, while neglecting the effect of etching of the natural fractures by acid and their contribution to the overall conductivity of the fracture system. There is a limited number of publications on the modeling of acid fracturing process in naturally fractured carbonate reservoirs. Mou et al. (2012) studied the leakoff mechanism during acid fracturing in naturally fractured carbonate oil reservoirs. They developed a mathematical model, in which a hydraulic fracture is intersected by two natural fractures. Acid is injected into the hydraulic fracture and leaks into the matrix through the hydraulic fracture wall, and into the natural fractures and then into the reservoir through the natural fracture walls. The etching of the hydraulic fracture and the increase of its width over time are neglected by the model. The authors studied the effect of acid concentration, natural fracture width and density, as well as formation permeability on leakoff. They concluded that acid leakoff is greater than inert fluid leakoff, and leakoff rate increases with increasing acid concentration. Also, they found that the acid leakoff through the matrix was negligible compared to

the leakoff through the natural fractures, and leakoff increased with increasing natural fracture width and density. The leakoff through the natural fractures was found to increase with time as the fractures being stimulated, and then decrease due to the compressibility effects. The similar study on the leakoff behavior in naturally fractured gas reservoirs (Xu et al. 2014) showed similar trends with the results obtained for the oil reservoir. It was found that the natural fractures leakoff could have more significant contribution to the total leakoff, and the matrix leakoff is negligible.

Overall, extensive work has been done in modeling of acid fracturing process and estimating acid fracture conductivity, but there is a lack of studies on modeling of acid fracturing in naturally fractured carbonate reservoirs and on investigating the effect of natural fractures on acid fracturing stimulation efficiency. This paper describes a new modeling approach that includes the presence of natural fractures in simulation of both acid fracturing and fractured well productivity. The results of simulating the acid fracturing treatment in a naturally fractured carbonate reservoir and evaluating the well productivity for a wide range of input parameters are presented in this work.

Methodology

The model developed in this study consists of an acid fracturing model coupled with a reservoir model. The acid fracturing model with natural fractures presented by Ugursal et al. (2018) is adopted in this study. The leakoff calculation method used in the coupled model described in this study is different from the Carter's leakoff model. The coupled model simulates fluid flow in a rectangular reservoir containing a fully-penetrating vertical well located in the center of the reservoir. The reservoir drainage region is only simulated to evaluate the acid leakoff and the fractured well productivity (a single-well model). The well is intersected by a bi-wing vertical fracture, which is intersected by multiple transverse symmetric natural fractures. The modeled domain represents one quarter of a reservoir domain (Figure 1). The fracture geometry is approximated as a channel between two parallel plates. A non-uniform gridding is adopted in the x- and y-directions with refined grid size near the intersection of the hydraulic fracture with the natural fractures and near the hydraulic fracture plane, respectively. Acid is injected through the hydraulic fracture entrance (perpendicular to the y-z plane). A portion of acid leaks through the hydraulic fracture walls (perpendicular to the x-z plane) and through the natural fracture walls (perpendicular to the y-z plane) into the reservoir, while the rest of acid exits through the hydraulic fracture tip.

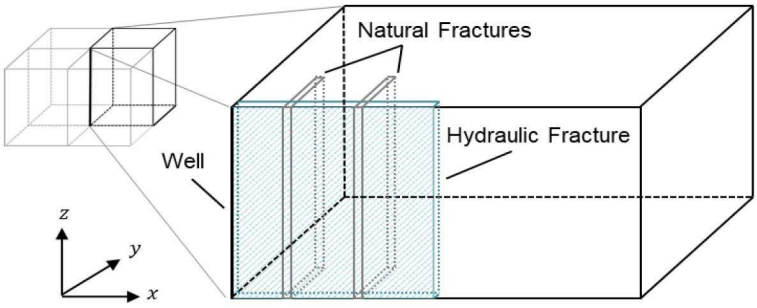

Figure 1—Model domain (not to scale)

For acid fracturing in a naturally fractured limestone reservoir, we can assume the steady state laminar flow of incompressible Newtonian fluid. This assumption holds for injection of straight acid into a fracture at injection rates typical for an acid fracturing treatment rates. Gravity effects are neglected by the model. We assume infinite acid/rock reaction rate, which is a valid assumption because of the fast reaction between concentrated hydrochloric acid with calcite. The model assumes that the pressure required to create a hydraulic fracture during pad injection is enough to open the existing natural fractures intersecting the hydraulic fracture. This assumption is only valid for low horizontal-stress contrast formations. For modeling

the fluid flow through porous media in the reservoir, we assume laminar flow of incompressible fluid. The model assumes single-phase flow in the reservoir neglecting water saturation effects.

The model does not simulate hydraulic fracture propagation during acid fracturing treatments. Instead, the model assumes the initial fracture geometry and the fixed fracture height and length throughout the pumping.

In the coupled model, fluid flow through porous media is simulated by solving the diffusivity equation (Eq. 1) in the reservoir drainage region with a fractured well. The diffusivity equation is solved during acid injection as a part of acid fracturing treatment to calculate leakoff, and during production of a fractured well to evaluate productivity. The diffusivity equation states,

$$\nabla \cdot (k \cdot \nabla p) = \phi \mu c_t \frac{\partial p}{\partial t}, \tag{1}$$

where k is permeability, p is pressure, ϕ is porosity, μ is fluid viscosity, and t is time. The initial and the boundary conditions are different during acid injection and during well production. The initial condition for acid injection assumes that pressure everywhere in the domain is equal to the initial reservoir pressure. The permeability is equal to the reservoir permeability, except for the fracture permeability, which is defined by the initial fracture width,w.

The initial conditions for acid injection are

$$\begin{aligned} &p(x,y,z) = p_i \;\; \forall x,y,z, \quad t = 0 \\ &k(x,y,z) = k_r \;\; x,y,z \notin \text{fracture}, \quad t = 0 \\ &k(x,y,z) = \frac{w^2}{12} \;\; x,y,z \in \text{fracture}, \quad t = 0 \end{aligned} \tag{2}$$

During the injection, the pressure at the well is equal to the downhole injection pressure, p_f, and a no-flow condition is assumed for the reservoir outer boundaries.

The boundary conditions during acid injection are

$$\begin{aligned} &p(x,y,z) = p_f \;\; x = 0, y = 0, \forall z, \quad t > 0 \\ &\frac{\partial p}{dx} = 0 \;\; x = L_x, \; \forall y,z, \; t > 0 \\ &\frac{\partial p}{dy} = 0 \;\; \forall x, y = L_y, \forall z, \; t > 0 \\ &\frac{\partial p}{dz} = 0 \;\; \forall x,y,z = h, \; t > 0 \end{aligned} \tag{3}$$

where L_x is half-length of the reservoir domain, L_y is half-width of the reservoir domain, and h is height of the reservoir domain. Permeability is equal to the reservoir permeability everywhere, except for the fracture, where the permeability is defined by the current fracture width which equals to the dynamic width, w, plus the etched width,w_e.

$$k(x,y,z) = \frac{(w+w_e)^3}{12} \;\; x,y,z \in \text{fracture} \tag{4}$$

Before production begins, the pressure in the reservoir is equal to the reservoir pressure achieved at the end of the acid injection. The permeability everywhere is equal to the reservoir permeability, except for the fracture permeability, which is defined by the fracture etched width and conductivity, which is calculated using the correlations developed by Deng et al. (2012).

Initial Conditions:

$$\begin{aligned} &p(x,y,z) = p_r \;\; \forall x,y,z, \quad t = 0 \\ &k(x,y,z) = k_r \;\; x,y,z \notin \text{fracture}, \quad t = 0 \\ &k(x,y,z) = k_f \;\; \forall x,y,z \in \text{fracture}, \quad t = 0 \end{aligned} \tag{5}$$

During production, the boundary condition at the wellbore is a constant flow rate, and no-flow boundary conditions are assumed for the reservoir outer boundaries. This leads to a pseudo-steady state condition after the initial transient flow.

Boundary Conditions:

$$\left(\frac{\partial p}{\partial x}\right)_{wellbore} = -\frac{qB\mu}{(wk_f)2h_f}$$
$$\frac{\partial p}{dy} = 0 \quad \forall x, y = L_y, \forall z, \ t > 0 \tag{6}$$
$$\frac{\partial p}{dz} = 0 \quad \forall x, y, z = h, \ t > 0$$

Production simulation performed in this study is time dependent, and productivity index stabilizes after initial transient flow, characterizing a pseudo-steady state. The metrics used in this study to compare different cases is dimensionless productivity index at pseudo-steady state, J_{Dpss}, which is calculated using the following expression (Economides et al. 2013):

$$J_{Dpss} = \frac{qB\mu}{2\pi\bar{k}h(\bar{p}-p_w)}, \tag{7}$$

where $\bar{p}$ is average pressure in the reservoir, p_w is pressure at the well, $\bar{k}$ is average permeability in the reservoir. The pressure and flow rate in Eq. 7 are provided by the simulation results from Eq. 1.

The coupled model calculates the leakoff by simulating acid flow through the porous medium in the direction perpendicular to the fracture walls (Figure 2). This approach yields more realistic estimate of the effect of leakoff on acid fractured well performance (Ugursal et al., 2018).

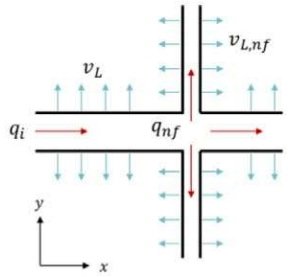

Figure 2—Acid leakoff schematics

The leakoff velocity is calculated as

$$v_L = -\frac{k}{B\mu}\frac{\partial p}{\partial y},$$
$$v_{L,\,nf} = -\frac{k}{B\mu}\frac{\partial p}{\partial x}, \tag{11}$$

where v_L and $v_{L,\,nf}$ are leakoff velocities for the hydraulic fracture and natural fracture leakoff, respectively, $\partial p/\partial x$ and $\partial p/\partial y$ are pressure gradients between the fracture and the reservoir in the x- and y-directions, respectively, k is permeability, μ is fluid viscosity, and B is formation volume factor.

The coupled model captures the leakoff rate as a function of time, and takes into account the interaction between natural fractures; hence, the coupled model does not impose the limitation on fracture spacing and allows leakoff rate of individual natural fractures to vary with fracture location and spacing. Also, the coupled model assumes that leakoff rate is restricted by the injection rate. At the beginning of acid injection, when the leakoff rate is high and researches the limit of the injection rate, the acid would not reach the tip of the hydraulic fracture and acid flow is unevenly distributed among the natural fractures. Acid propagation along the hydraulic fracture depends on the leakoff rate change over time. The natural fractures located

closer to the hydraulic fracture inlet at the wellbore receive acid earlier than the fractures located further away from the hydraulic fracture entrance.

The model workflow is presented in Figure 3 and is described as follows. First, the input parameters, such as hydraulic and natural fracture geometry, natural fracture spacing, reservoir properties, acid fracturing treatment conditions, and other parameters are defined. Then, the gridding along the hydraulic fracture length is implemented based on the natural fracture spacing. After that, the gridding of the rest of the reservoir domain is applied. After the model initiation, it simulates the acid flow in the fracture system and the acid leakoff through the fracture walls into the reservoir assuming a constant pressure at the well that equals to the pressure at the hydraulic fracture inlet. Based on the obtained leakoff velocities, the pressure distribution in the hydraulic fracture is obtained. The updated value of the pressure at the fracture inlet is compared with the assumed value and the iteration process is repeated until convergence is obtained. Then, the acid concentration distribution in the hydraulic fracture is obtained, and the etched width of the hydraulic and the natural fractures is calculated for each time step. The permeability of the fractures is calculated from the fracture width and is updated at each time step. At the end of the acid injection, the fracture conductivity is estimated based on the final etched width achieved during the injection, using the correlations by Deng et al. (2012). After the acid injection is finished, the model simulates the reservoir fluid flow from the reservoir into the well producing at a constant flowrate. Pressure in the reservoir is calculated and updated during each time step. When the reservoir reaches the pseudo-steady state, the productivity index is estimated.

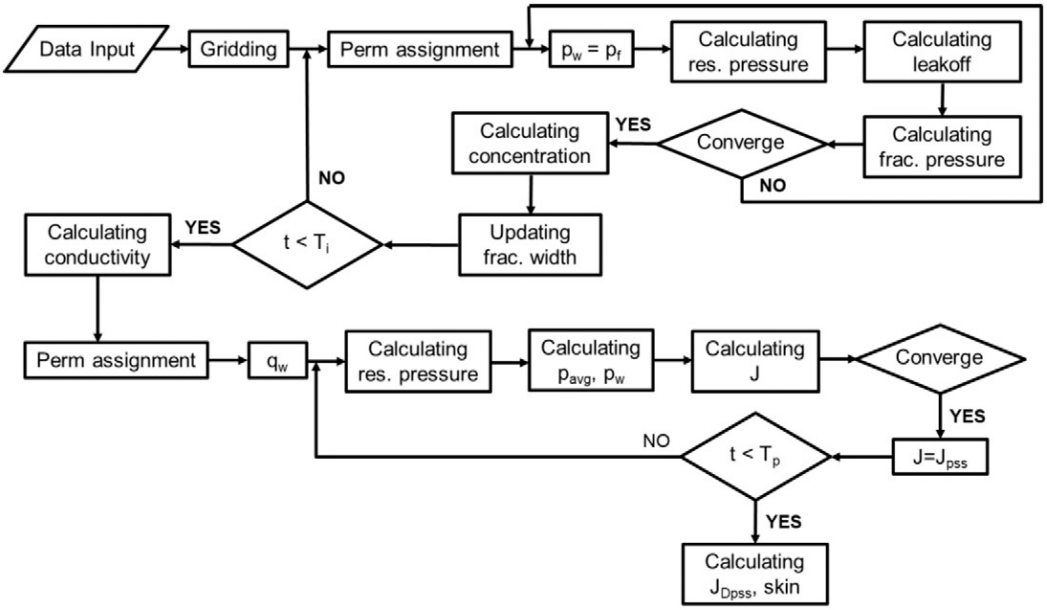

Figure 3—Model workflow

Simulation Results

A series of cases were simulated by using the coupled model to demonstrate the capabilities of the model and to investigate the effect of various parameters, such as natural fracture properties, reservoir permeability, and treatment conditions on the efficiency of acid fracturing stimulation. The stimulation efficiency was estimated based on the generated well productivity and skin factor. To evaluate the impact of natural fractures on the acid fracturing performance, the results were compared to the base case scenario, which corresponds to acid fracturing stimulation and production in a reservoir without natural fractures.

Leakoff Behavior during Acid Fracturing

The effect of leakoff on acid fracturing process and productivity after fracturing was first examined in this study. As the new model has the ability to simulate individual natural fractures with independent leakoff behavior, we set up a base case that contains a hydraulic fracture and multiple natural fractures. The simulation domain is one quarter of the reservoir domain, with a wellbore located at the origin (also referred as the entry of hydraulic fracture), as shown in Figure 4a. The input parameters for the simulation are summarized in Table 1. In the base case, for a given length of the hydraulic fracture and a given natural fracture spacing, there are three natural fractures intersecting the hydraulic fracture.

Leakoff rate of individual natural fractures depends on their location and natural fracture spacing. Figure 4b shows the top view of the pressure field at the end of the acid injection. As can be seen from Figure 4b, the pressure distribution in the reservoir around the fracture system is not uniform. There are higher pressure regions along the hydraulic fracture and along the natural fractures, which is associated with the leakoff from the fractures into the reservoir. The position of the spike-shaped regions of higher pressure coincides with the natural fractures location, and the extension of those spikes into the reservoir is determined by the leakoff intensity of the individual natural fractures over time.

Table 1—Input parameters for simulation to study the acid leakoff behavior

Parameter	Value
Hydraulic fracture properties	
Length	150 ft
Height	70 ft
Width	0.1 in
Natural fracture properties	
Length	50 ft
Height	70 ft
Width	0.01 in
Spacing	40 ft
Reservoir properties	
Size	1640 ft × 1640 ft
Porosity	0.15
Permeability	10 md
Closure stress	1500 psi
Treatment conditions	
Injection rate	20 bpm
Injection Time	20 min
Acid type & concentration	HCl 15wt%

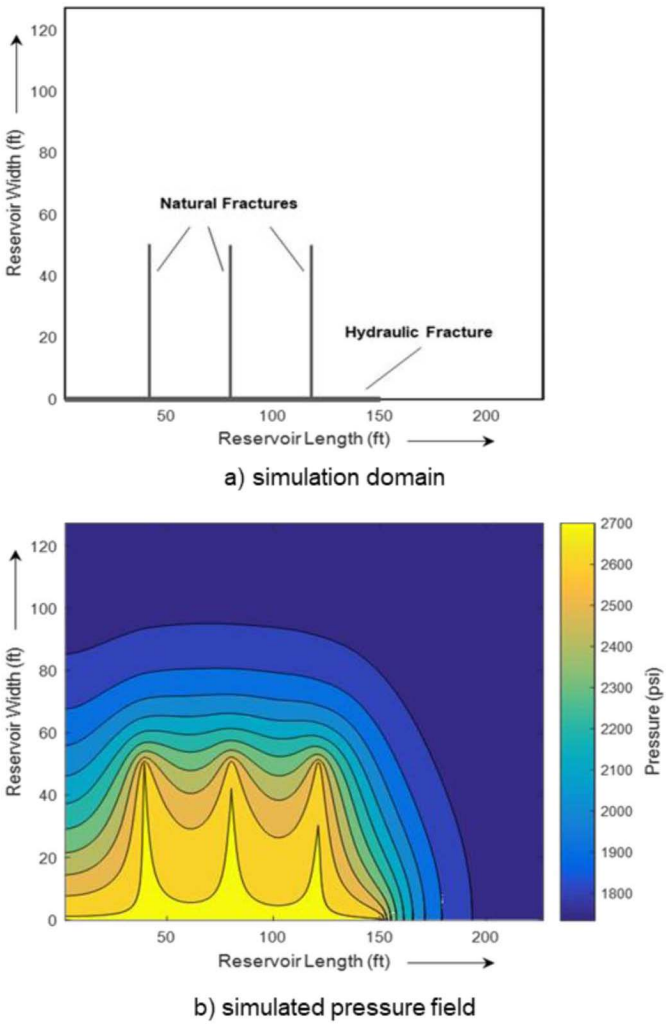

Figure 4—Reservoir pressure distribution at the end of acid injection (on the top) and corresponding location of the hydraulic fracture and the natural fractures (on the bottom)

Figure 5 plots the effective leakoff rate as a function of location along the fracture for each natural fracture. The simulation result shows that acid does not leak off uniformly across the fracture walls as assumed by the Carter's leakoff model. In contrast, the leakoff rate increases significantly towards the natural fracture tip, which is caused by a larger pressure difference between the fracture and the undisturbed reservoir beyond the fracture tip compared to the pressure difference between the fracture and the reservoir region bounded by the neighboring natural fractures, as illustrated in Figure 4. The reservoir pressure in the region between the natural fractures builds up fast because of its relatively small volume and large leakoff area. The reservoir pressure beyond the fracture tip increases more slowly due to a large volume of the virgin reservoir adjacent to the fracture tip and a small leakoff area.

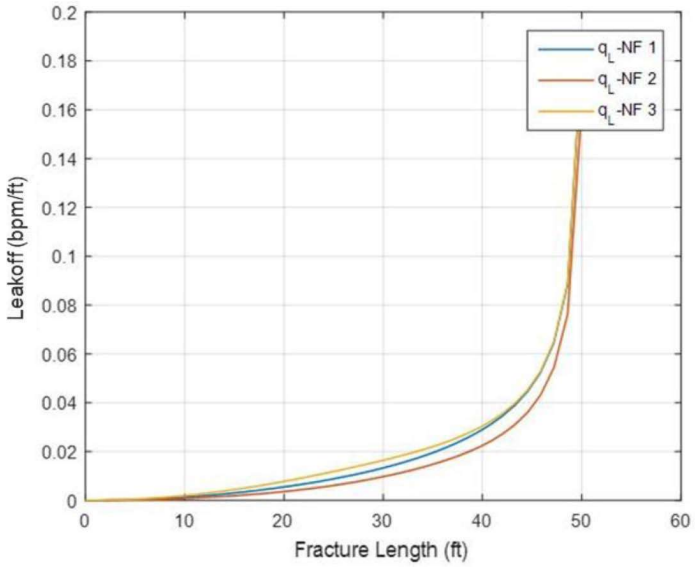

Figure 5—Leakoff from individual natural fractures at the end of acid injection

Unlike predicted by the Carter model, leakoff does not always decrease with time. It may increase during the initial time of acid injection, as shown in Figure 6. This happens as the natural fractures are stimulated by the acid. The leakoff flowrate behavior is associated with the acid loss from the hydraulic fracture and from the individual natural fractures as a function of time. The total leakoff rate is limited by the injection rate. The reduction of the leakoff rate from the hydraulic fracture is accompanied by the proportional increase of the leakoff rate from the natural fractures. Hence, the hydraulic fracture leakoff curve mirrors the natural fracture leakoff curve during the initial time of acid injection. Later in time, both the hydraulic fracture and the natural fracture leakoff rates decrease with time following the trend described by the Carter model. This is due to the fact that after initial stimulation the natural fracture conductivity becomes infinitely large compared to the reservoir permeability, and the fluid loss is dictated by the reservoir fluid compressibility. The three peaks on the natural fracture leakoff curve (Figure 6) are associated with stimulation of the first, the second, and the third natural fractures, respectively.

In order to better understand this behavior, the leakoff rate of the individual natural fractures as a function of time is presented in Figure 7. As can be seen from this figure, the leakoff from the natural fractures increases initially as the fractures being stimulated, and then decreases. The reduction in leakoff rate is proportional to the decrease in the pressure difference between the fracture and the reservoir caused by the acid leakoff. Also, the leakoff from the natural fractures happens sequentially in the order of the natural fracture location relative to the hydraulic fracture inlet. Thus, at the beginning of the acid injection, when the total leakoff rate is high and is restricted by the injection rate, the leakoff happens only through the part of the hydraulic fracture and the first natural fracture. After about 1 minute, when the total leakoff rate decreases below the injection rate, acid propagates further away from the hydraulic fracture entrance and leaks into the second natural fracture. The leakoff initiation from the third natural fracture corresponds to the reduction of the total leakoff rate below the injection rate from the fracture system located upstream.

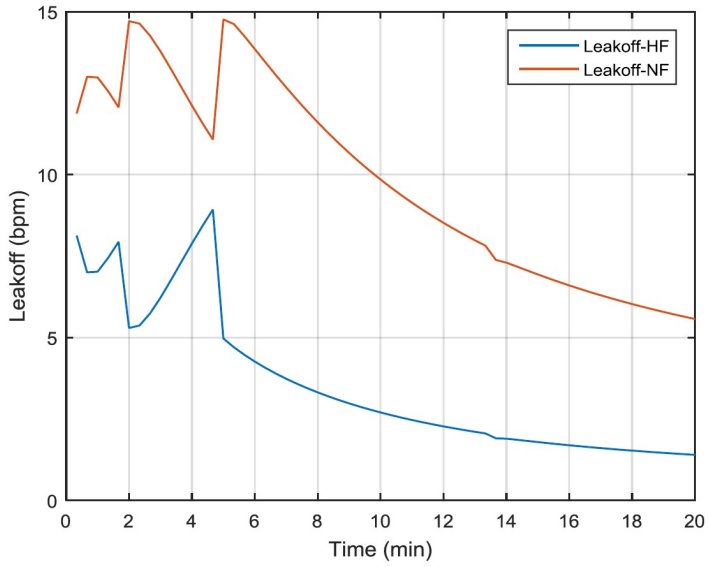

Figure 6—Total leakoff from hydraulic fracture and from natural fractures

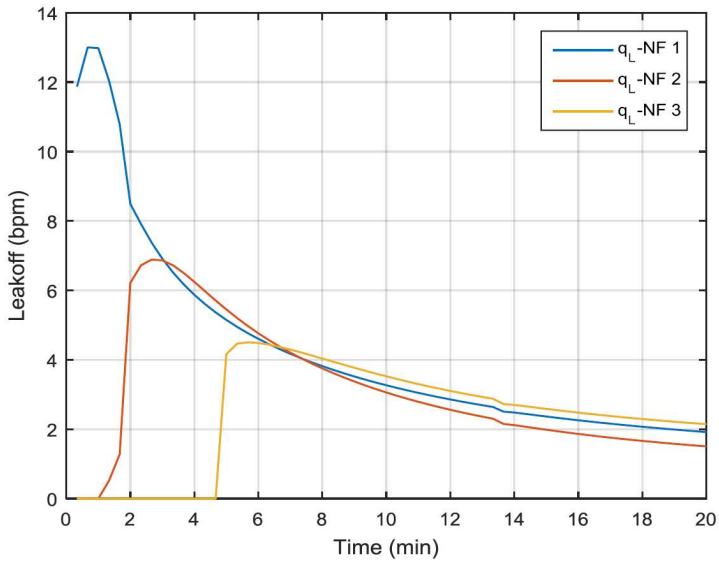

Figure 7—Leakoff from individual natural fractures over time

As was mentioned before, leakoff not only depends on natural fracture location but also on fracture spacing. The simulation is conducted for the case when all the parameters are kept the same as in the previous example but the natural fracture spacing is reduced from 40 ft to 10 ft. For a given length of the hydraulic fracture, with the spacing of 10 ft, there are 14 natural fractures present. The reservoir pressure distribution at the end of injection for this case is shown in Figure 8. The result indicates that for more closely spaced natural fractures the pressure distribution between the fractures is uniform at the end of stimulation because of higher leakoff from the natural fractures compared with the case of lower density network of natural fractures.

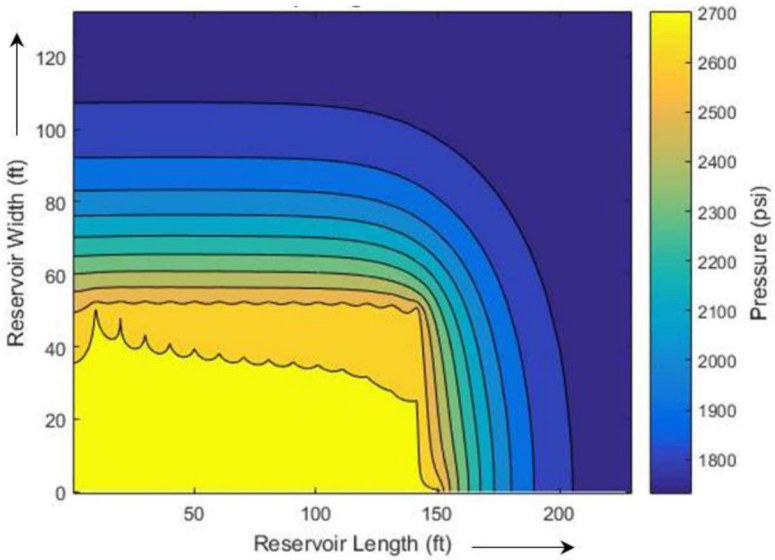

Figure 8—Reservoir pressure distribution at the end of acid injection for the case of natural fracture spacing of 10 ft

Effect of Natural Fracture Properties

Several cases are simulated to investigate the effect of natural fracture width, length, and spacing on the acid fracturing stimulation efficiency in naturally fractured reservoir. The parameters, such as the hydraulic fracture geometry, the treatment conditions, and the closure stress are held constant for all the simulation cases. The input parameters are summarized in Table 2. The stimulation efficiency is defined by the productivity index ratio after stimulation to the one before stimulation, J/J_o which characterizes the folds of increase in well productivity due to the stimulation.

Table 2—Input parameters for simulation to study the effect of natural fracture properties and treatment conditions on well productivity

Parameter	Value
Hydraulic fracture properties	
Length	700 ft
Height	100 ft
Width	0.1 in
Reservoir properties	
Size	1640 ft × 1640 ft
Porosity	0.15
Closure stress	1500 psi
Treatment conditions	
Injection rate	16 bpm
Injection Time	25 min
Acid type & concentration	HCl 15wt%

Natural Fracture Width. In this study, we assume that a hydraulic fracture with a dynamic width is created by injecting a pad fluid prior to acid injection. We also assume that the existing natural fractures intersecting the hydraulic fracture open during pad injection and have certain length, height, and dynamic width. The width of natural fractures can be smaller than or equal to the hydraulic fracture width. The initial fracture geometry serves as an input to the coupled model to simulate acid fracturing. The cases are modeled with

the dynamic width of natural fractures varying from 0.005 to 0.01 to 0.1 inches. All cases assume that all the natural fractures have equal width. The length and the height of the natural fractures are held constant and equal to 50 ft and 100 ft, respectively for all the cases in study. The natural fracture spacing is set to 50 ft, which corresponds to 13 natural fractures intersecting the hydraulic fracture with the given length of 700 ft.

Figure 9 plots the productivity index ratio as a function of natural fracture width. It also shows the productivity index ratio for the case when there are no natural fractures. It is observed that the dynamic width of the natural fractures has a negligible effect on stimulation efficiency. This is due to the fact that the hydraulic fracture conductivity has a dominant effect on the productivity, and the conductivity of the main fracture is negligibly affected by the natural fracture width. For the cases simulated, the acid fracturing stimulation efficiency is greater in a naturally fractured reservoir compared to the reservoir without natural fractures. This is because the acid loss into the natural fractures does not affect the conductivity of the main fracture and generates additional conductivity by etching the natural fractures.

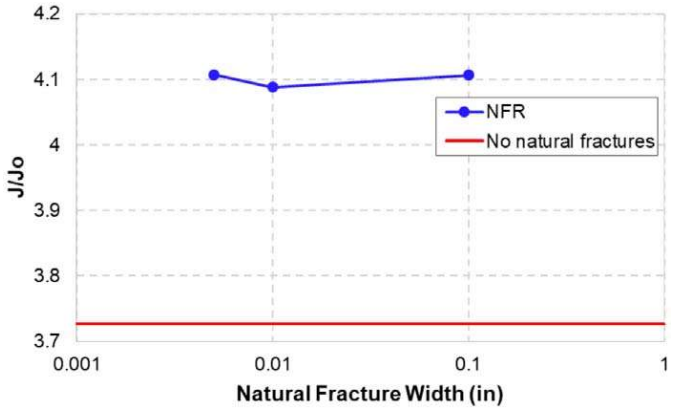

Figure 9—Effect of natural fracture width on stimulation efficiency

Natural Fracture Length. In naturally fractured formations, each fracture can be either isolated or interconnected to form a fracture network. To model both scenarios, several cases are simulated with the natural fracture length varying from 10 ft, representing short natural fractures, up to 100 ft, representing either long fractures or several short fractures connected into a fracture network. The natural fracture height and width are constant for all the simulation cases and are set to 100 ft and 0.01 inches, respectively. The natural fracture spacing is 50 ft, which corresponds to 13 natural fractures intersecting the 700-ft long hydraulic fracture.

Figure 10 shows that with increasing length of the natural fractures the productivity ratio drops, indicating a decreased stimulation efficiency. As natural fracture length increases, the area exposed to leakoff increases, resulting in a higher acid loss into the natural fractures. With increased leakoff, there is less acid available to etch the main fracture, resulting in a lower conductivity. In addition, with increasing fracture length and increasing leakoff, the acid transport along the hydraulic fracture is limited. Hence, live acid does not reach all the natural fractures, leaving some of them unstimulated. More etching occurs in the natural fractures located closer to the hydraulic fracture entry towards the wellbore.

Figure 10 also shows the comparison of low-permeability reservoir (1 mD, Figure 10a) and high-permeability reservoir (10 md, Figure 10b). The decline rate of productivity index ratio is greater for the low permeability reservoir case (Figure 10a) compared with the high permeability reservoir (Figure 10b). The total leakoff is lower in low-perm rock compared with high-perm rock. Therefore, in low permeability reservoirs, acid is received by a higher number of natural fractures during acid injection. For low permeability formations, the increase of fracture length has a greater effect on productivity reduction than in high permeability reservoirs.

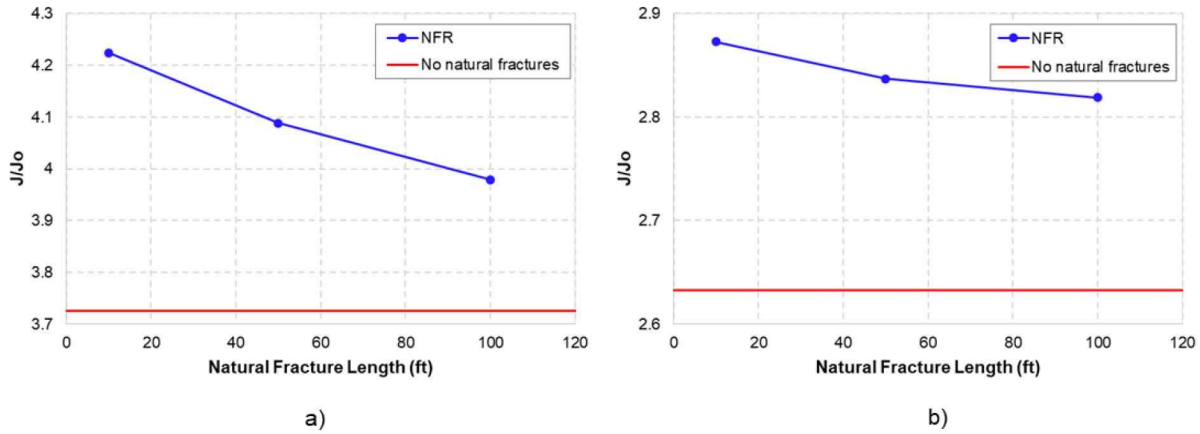

Figure 10—Effect of natural fracture length on productivity in low permeability (a, 1 mD) and high permeability (b, 10 mD) rocks.

Natural Fracture Spacing. Natural fracture spacing is an important parameter that characterizes the density of a fracture network and affects the performance of acid fracturing treatments. In carbonate formations fracture spacing may vary significantly from less than a foot to tens or even hundreds of feet. To study the effect of natural fracture spacing on productivity, several cases were simulated with the spacing varying from 10 ft to 100 ft and all the other parameters being constant.

The result of effect of natural fracture spacing on productivity is presented in Figure 11. Figure 11 also shows the case of the reservoir without natural fractures. For a given fracture geometry and treatment conditions, there is an optimum natural fracture spacing that yields the highest productivity increase. In high-density (10-ft spacing, 69 natural fractures) and low-density (100-ft spacing, 10 natural fractures) natural fracture cases, the production improvements are relatively low. The optimal condition for the simulated case is 50-ft spacing, or 13 natural fractures. At low spacing or high fracture density, leakoff increases because of higher exposure of acid to natural fractures, and, as a result, the etching of hydraulic fracture decreases. At high spacing or low fracture density, the conductivity contribution from natural fractures reduces. The conductivity of the hydraulic fracture and the natural fractures should be balanced for high productivity improvement. The optimal condition changes with reservoir properties and injection conditions. When designing an acid fracture treatment, the natural fracture density estimated from geological information can be used for a sensitivity study to determine the optimal treating condition.

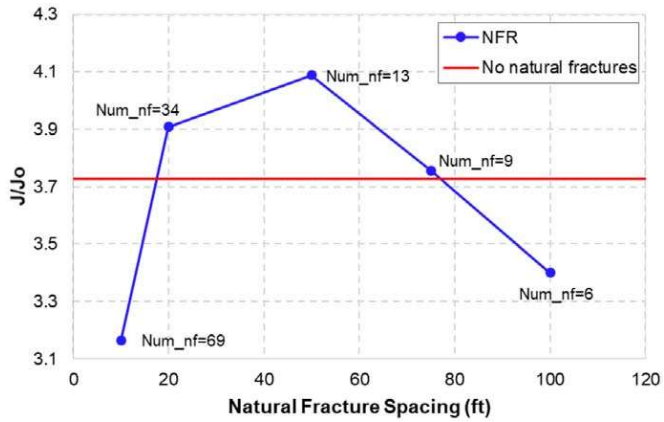

Figure 11—Effect of natural fracture spacing on stimulation efficiency in low permeability (1 md) reservoir

Figure 12 illustrates the pressure distribution in the reservoir at the end of the treatment for different fracture spacing. For the case of closely spaced natural fractures, the reservoir pressure in the region between

neighboring fractures builds up fast and becomes almost uniform at the end of stimulation due to high leakoff and small reservoir volume bounded by the neighboring fractures. As the spacing increases, the region of undisturbed reservoir pressure between the natural fractures becomes larger. Therefore, the fracture spacing not only affects the total leakoff into the natural fractures but also the leakoff of individual natural fractures resulting from the pressure change in the reservoir caused by leakoff.

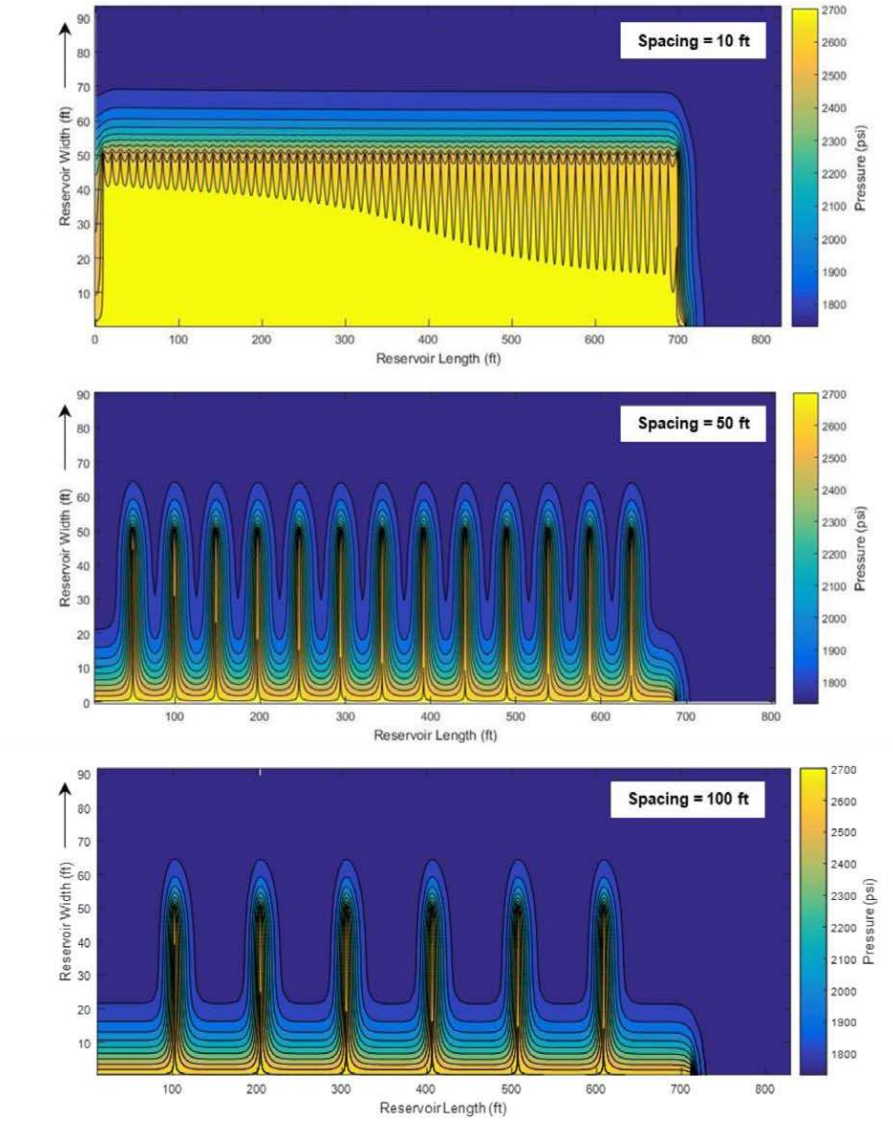

Figure 12—Reservoir pressure distribution at the end of acid injection for various natural fracture spacing (top view)

Effect of Treatment Conditions

The efficiency of acid fracturing stimulation can be improved by optimizing treatment design. There are several design parameters that can be tuned to increase the post-stimulation productivity, and those include type of acid system, acid concentration, injection rate, and volume of acid. Here, the influence of injection rate and volume of injected acid on the acid fracturing stimulation performance are analyzed.

Injection Rate. The effect of the acid injection rate on productivity was investigated by simulating the cases with the rate varying from 10 bpm to 16 bpm to 20 bpm. The total volume of acid injected is fixed at 400 bbl, the natural fracture spacing is 50 ft and the natural fracture length is 100 ft, and these parameters are kept constant for all the simulation cases.

Figure 13 shows the productivity index ratio as a function of injection rate for the low-permeability and high-permeability reservoirs. The results are compared against the case of a reservoir without natural fractures to evaluate the efficiency of acid fracturing treatments in naturally fractured reservoirs. It is observed from Figure 13 that in low permeability reservoir the post-stimulation productivity increases with increasing pumping rate for both the naturally fractured reservoirs and the reservoirs without natural fractures. As injection rate increases, acid penetration distance increases, generating longer effective length for hydraulic fracture. Also, with increased pumping rate, the leakoff into the natural fractures increases, resulting in a greater etching and a higher conductivity of the natural fractures, as well as a higher number of stimulated natural fractures.

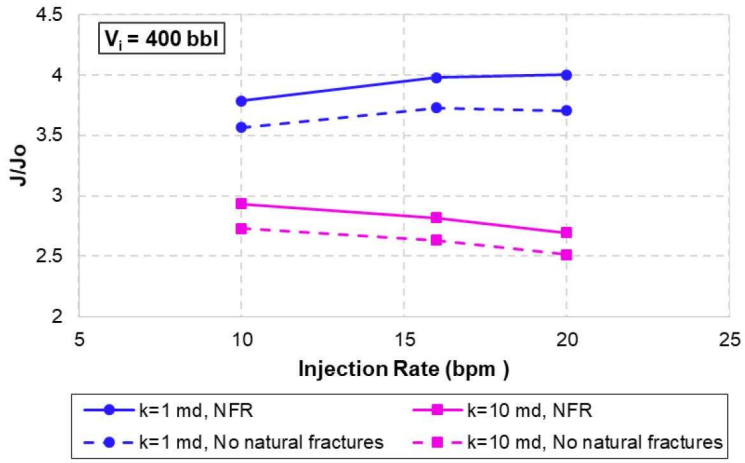

Figure 13—Effect of injection rate on stimulation efficiency

In contrast to the low-permeability formation, the stimulation efficiency decreases with increasing injection rate in the high-permeability formation, and the trend is the same for the reservoir containing natural fractures and the reservoir with no natural fractures present. When formation permeability is high, acid loss by leakoff is also high. Most acid leaks off into the formation through the walls of the hydraulic fracture (in case of a reservoir without natural fractures) or both the hydraulic fracture and the natural fractures located close to the hydraulic fracture entrance (in case of a naturally fractured reservoir). This can reduce the conductivity of hydraulic fracture at the region close to the wellbore. As proved in propped hydraulic fracturing, in high permeability reservoirs, a higher fracture conductivity is needed to obtain the optimum dimensionless fracture conductivity. Highly conductive shorter fracture is preferred over a long fracture with lower conductivity. The lower injection rate results in a shorter effective fracture length, with higher conductivity near the fracture entrance, yielding a higher productivity in high permeability reservoirs. The injection rate must still be high enough to propagate a fracture and keep it open during acid injection. The performance of acid fracturing treatment in a naturally fractured reservoir is better than in a reservoir without natural fractures because of the additional conductivity generated by the etching of natural fractures.

The effect of reservoir permeability on the leakoff behavior is illustrated in Figure 14 through the pressure field plots at the end of acid injection for low-permeability (top picture) and high-permeability (bottom picture) naturally fractured reservoirs. With increasing permeability, the leakoff increases, and the natural fractures start communicating with each other. As can be seen from Figure 14, at the end of the stimulation treatment in the low-permeability reservoir, there exists regions between the natural fractures where pressure is not disturbed by injection; while in the high-permeability formation the reservoir pressure everywhere near the fracture network is higher than the initial pressure.

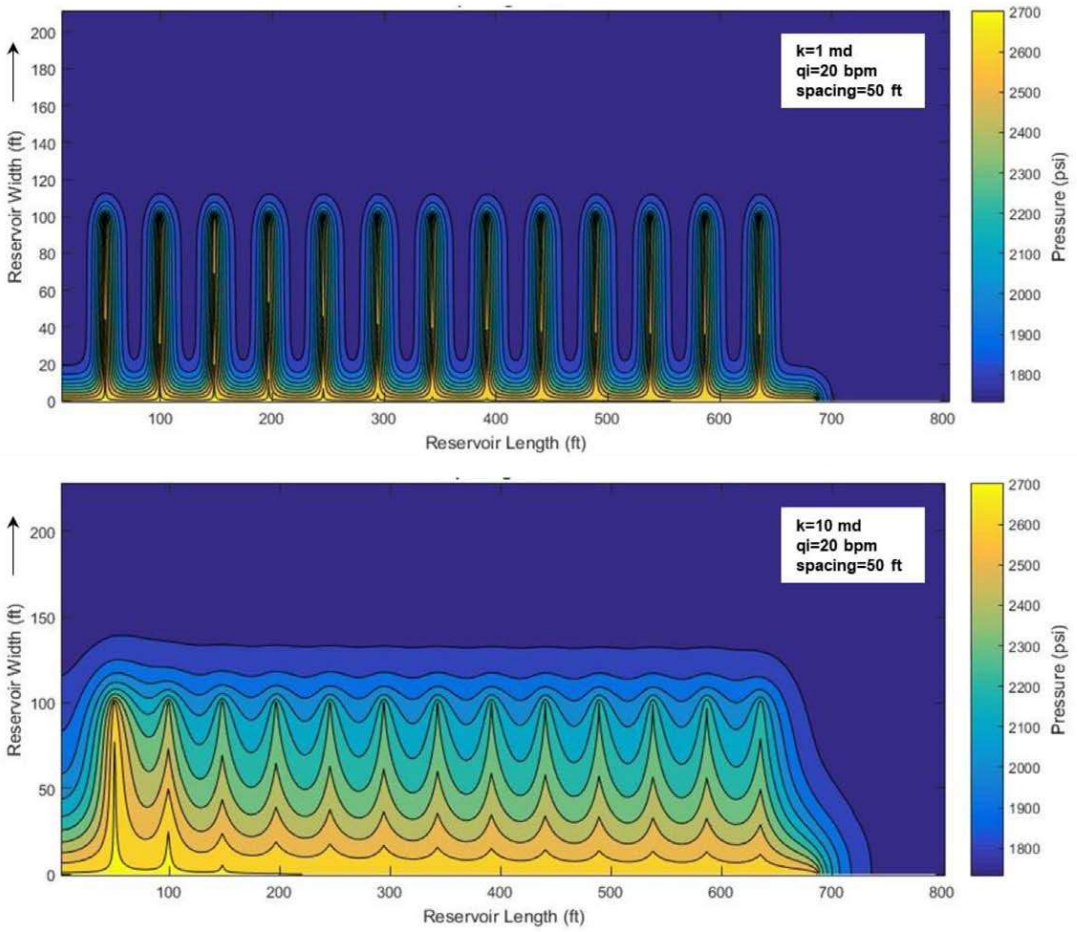

Figure 14—Top view of reservoir pressure distribution at the end of acid injection in low permeability (top) and high permeability formation (bottom)

Volume of Acid. The effect of acid volume on productivity increase is studied by simulating the cases with 800 bbls of total injected acid. All the other inputs are the same as the ones used to investigate the effect of injection rate. The results are presented in Figure 15. Figure 15 should be compared with Figure 13 for injection volume effect. It shows that a greater productivity improvement is achieved when the acid volume is increased, as expected, for both low-perm and high-perm cases. In constrast to the results in Figure 13, the productivity index ratio increases as the injection rate increases for both the low-perm and the high-perm reservoirs when the acid volume is doubled (Figure 15). The rate of increase in productivity index ratio is greater in the low-permeability formation (steeper slope) compared with the high-permability case. For the high-permeability reservoir, the post-stimulation productivity slightly increases with the pumping rate increasing from 10 to 16 bpm, and then decreases when the injection rate increases to 20 bpm when a higher volume of acid is injected (Figure 15), while the mono-decreasing trend is observed for the case of a lower total injection volume (Figure 13). This can be attributed to the fact that a smaller injection rate results in a shorter and more conductive main fracture, while a higher pumping rate yields a longer but a less conductive fracture. When the injection rate increases from 10 bpm to 16 bpm, the effective length of the hydraulic fracture increases without a significant decrease in fracture conductivity, resulting in a productivity increase. Then, when the injection rate increases from 16 bpm to 20 bpm, the gain in fracture length does not compensate the loss in conductivity resulting in the productivity reduction. For this case, the optimum injection rate is close to 16 bpm. Similar to the case with a lower injected volume, the presence of the natural fractures enhances the acid fracturing stimulation performance compared to the reservoir without natural fractures.

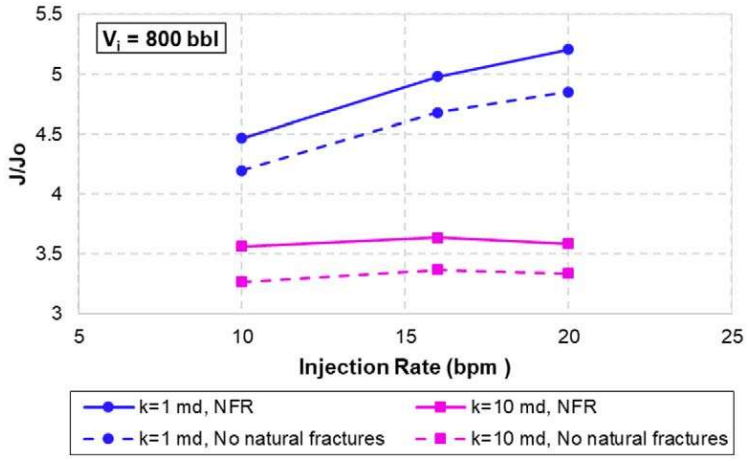

Figure 15—Effect of injection rate on stimulation efficiency

Conclusions

The acid fracturing model coupled with the reservoir model presented in this study enables simulation of acid fracturing treatment and production in naturally fractured carbonate reservoirs. The new model accounts for acid flow and reaction, and conductivity generation in both hydraulic fracture and natural fractures. The model simulates a realistic leakoff behavior during acid injection by modeling the acid flow through porous media from fractures into reservoir, instead of assuming a constant leakoff rate reduction. The model accounts for the interaction among natural fractures during acid injection, so that the leakoff of individual natural fractures depends on their location and natural fracture spacing. The results of this study can be used to design and optimize acid fracturing treatments in naturally fractured carbonate reservoirs. The following conclusions are reached based on the simulation results:

- Conductivity of hydraulic fracture has a dominant effect on the productivity. However, the presence of natural fractures can enhance acid fracturing stimulation efficiency by contributing to the overall conductivity.
- Natural fracture initial width has a negligible effect on acid fracturing performance.
- Post-stimulation productivity decreases with increasing natural fracture length.
- There is an optimum condition for each defined natural fracture system that yields the greatest stimulation efficiency.
- Productivity can be increased by increasing the injection rate in low permeability reservoirs. However, the results can be opposite in high permeability reservoirs.

Nomenclature

A	cross-sectional area
B	formation volume factor
c_t	total compressibility of the reservoir
C_L	total leakoff coefficient
h_f	height of the fracture
J_D	dimensionless productivity index
J_{Dpss}	dimensionless productivity index at pseudo-steady state
k	permeability of the formation
$\bar{k}$	average permeability of the formation
k_f	permeability of the fracture

L_x length of the reservoir
L_y width of the reservoir
p pressure as a function of position
$\bar{p}$ average pressure in the reservoir
p_e back-pressure
p_f pressure in the fracture
p_i initial pressure in the reservoir
p_m pressure in the rock matrix
p_r pressure in the reservoir
p_w pressure at the well
q flow rate
r_e drainage radius of the reservoir
r_w wellbore radius
s skin factor
t cumulative time of injection
t_{pss} time to reach pseudo-steady state flow
t_{DApss} dimensionless time to reach pseudo-steady state flow
v_L leakoff velocity
w width of the fracture
$\bar{w}$ average width of the fracture
w_e etched width of the fracture
wk_f conductivity of the fracture
μ viscosity of the reservoir fluid
σ_h minimum horizontal stress
ϕ porosity of the formation

References

Dake, L. P. 1978. *Fundamentals of Reservoir Engineering*, first edition. Elsevier.

Deng, J., Mou, J., Hill, A. D. et al. 2012. A New Correlation of Acid–Fracture Conductivity Subject to Closure Stress. *SPE Prod & Oper* **27** (2): 158–169. SPE-140402-PA. http://dx.doi.org/10.2118/140402-PA.

Economides, M. J., Hill, A. D., Ehlig-Economides, C. et al. 2013. *Petroleum Production Systems*, second edition. Westford, MA: Prentice Hall.

McCartney, E., Al-Othman, M., Alam, A. et al. 2017. Enhanced Acid Fracturing with Improved Fluid Loss Control and Near Wellbore Diversion Increases Production in Kuwait. Presented at the SPE Annual Technical Conference and Exhibition, San Antonio, Texas, 9-11 October. SPE-187444-MS. http://dx.doi.org/10.2118/187444-MS.

Mou, J., Zhu, D., and Hill, A. D. 2010. Acid-Etched Channels in Heterogeneous Carbonates - A Newly Discovered Mechanism for Creating Acid-Fracture Conductivity. *SPE J.* **15** (2): 404–416. SPE-119619-PA. https://doi.org/10.2118/119619-PA.

Mou J., Zhang, S., and Shang, Y. 2012. *Transp Porous Med* (2012) **91**: 573–584. Acid Leakoff Mechanism in Acid Fracturing of Naturally Fractured Carbonate Oil Reservoirs. http://dx.doi.org/10.1007/s11242-011-9860-4.

Oeth, C. V., Hill, A. D., and Zhu, D. 2014. Acid Fracture Treatment Design with Three-Dimensional Simulation. Presented at the SPE Hydraulic Fracturing Technology Conference, The Woodlands, Texas, 4-6 February. SPE-168602-MS. https://doi.org/10.2118/168602-MS.

Rahim, Z., Al-Kanaan, A. A., Kayumov, R. et al. 2017. Sequenced Fracture Degradable Diverters Improve Efficiency of Acid Fracturing in Multiple Perforated Intervals Completion Assembly. Presented at the Abu Dhabi International Petroleum Exhibition and Conference, Abu Dhabi, UAE, 13-16 November. SPE-188187-MS. https://doi.org/10.2118/188187-MS.

Romero, J., Gu, H., and Gulrajani, S. N. 2001. 3D Transport in Acid-Fracturing Treatments: Theoretical Development and Consequences for Hydrocarbon Production. *SPE Prod & Fac* **16** (2): 122–130. SPE-72052-PA. https://doi.org/10.2118/72052-PA.

Settari, A., Sullivan, R. B., and Hansen, C. 2001. A New Two-Dimensional Model for Acid-Fracturing Design. *SPE Prod & Fac* **16** (4): 200–209. SPE-73002-PA. https://doi.org/10.2118/73002-PA.

Ugursal, A., Zhu, D., and Hill, A. D. 2018. Development of Acid Fracturing Model for Naturally Fractured Reservoirs. Presented at the SPE Hydraulic Fracturing Technology Conference and Exhibition, The Woodlands, Texas, 23-25 January. SPE-189834-MS. https://doi.org/10.2118/189834-MS.

Williams, V., McCartney, E., and Nino-Penaloza, A. 2016. Far-Field Diversion in Hydraulic Fracturing and Acid Fracturing: Using Solid Particulates to Improve Stimulation Efficiency. Presented at the SPE Asia Pacific Hydraulic Fracturing Conference, Beijing, China, 24-26 August. SPE-181845-MS. https://doi.org/10.2118/181845-MS.

Xu, L., Zhang, S., and Mou, J. 2014. Acid Leakoff Mechanism in Acid Fracturing of Naturally Fractured Carbonate gas Reservoirs. *Adv Mat Res* **868** (2014): 682–685.